A Hybrid Moment Method/Finite-Difference Time-Domain Approach to Electromagnetic Coupling and Aperture Penetration into Complex Geometries

ALLEN TAFLOVE, MEMBER, IEEE, AND KORADA UMASHANKAR, SENIOR MEMBER, IEEE

Abstract—**An approach is presented for the direct modeling of electromagnetic penetration problems which involves a hybrid technique combining the frequency-domain method of moments (MM) and the finite-difference time-domain (FD-TD) method. The hybriding is based upon a novel use of a field equivalence theorem due to Schelkunoff, which permits a field penetration problem to be analyzed in steps by treating the relatively simple external region and the relatively complex internal region separately. The method involves first, determination of an equivalent short-circuit current excitation in the aperture regions of the structure using MM for a given external illumination. This equivalent current excitation over the aperture is next used to excite the complex loaded interior region, and the penetrating fields and induced currents are computed by the FD-TD method. A significant advantage of this frequency domain/time domain hybriding is that no Green's function need be calculated for the interior region. This hybrid approach takes advantage of the ability of MM to solve exterior problems using patch models and also takes advantage of the ability of FD-TD to model in great detail localized space regions containing metal structures, dielectrics, permeable media, anisotropic or nonlinear media, as well as wires.**

I. INTRODUCTION

ELECTROMAGNETIC penetration problems are difficult to treat with many analytical or numerical methods because of the inability of these methods to deal simply with the effects of structure apertures, curvatures, corners, and internal contents. Usually only relatively simple geometries and apertures are studied in an attempt to gain insight into the key penetration mechanisms and to allow an indirect estimate of the penetration for more complicated problems.

The problem of the penetration and coupling of electromagnetic energy through an aperture has been studied extensively by many investigators using analytical and method of moments (MM) numerical approaches [1] to characterize the behavior of simple aperture shapes in a conducting screen [2]–[6] or in a finite scattering body [7], [8]. However the analysis becomes very complicated if there are other scattering objects in the vicinity which are coupled to the aperture [9]–[12] wherein the mutual interaction must be fully taken into account. One powerful alternate approach is the pure finite-difference time-domain (FD-TD) method [13]–[17] which allows computation of the penetrated internal electromagnetic fields by direct modeling of the object of interest, including apertures and internal contents. However the pure FD-TD method is best suited for modeling localized regions. When such a region is part of a larger structure that is significantly affected by the electromagnetic excitation, it becomes difficult to account for the physics of the entire coupling problem using a single FD-TD model having a constant space lattice cell size. In fact, electromagnetic coupling problems involving the need to account simultaneously for the effects of both large and small spatial details (the "global–local problem") have been difficult to structure with any single analytical or numerical technique.

This paper presents an alternative approach for the direct modeling of electromagnetic penetration problems. This approach involves a hybrid technique combining the frequency-domain method of moments (MM) and the finite-difference time-domain (FD-TD) method. The hybriding is based upon a novel use of a field equivalence theorem due to Schelkunoff [18] which permits a field penetration problem to be analyzed in steps by treating the relatively simple external region and the relatively complex internal region separately. The method involves first, determination of an equivalent short-circuit current excitation in the aperture regions of the structure of interest using MM for a given external illumination. The computed equivalent current excitation over the aperture is next used to excite the complex loaded interior region, and the penetrating fields and induced current are computed by the FD-TD method [19], [20]. This hybrid method is also applicable when wires or material bodies are present in the interior region and coupled strongly to the aperture. An advantage of this frequency domain/time domain hybriding is that *no* Green's function need be calculated for the interior region. A further advantage of this hybrid approach is that it permits the treatment of those structures that are simultaneously electrically large compared to a wavelength and penetrated by locally complex cavity-backed apertures having dimensions comparable to a wavelength. Such structures requiring resolution of both large and small details at the same time have not been well-treated by any one previous analytical or numerical approach.

II. THE PURE FD-TD METHOD

The FD-TD method is ideal for the interior-field computations as discussed in [13]–[16] since it is capable of incorporating great detail into its model in a simple manner and without exhausting the resources of available computers. For example, in recent work the FD-TD method has been shown capable of accurately solving for hundreds of thousands of unknown field components within a few minutes of an array-processing computer (Control Data Cyber 203).

The FD-TD method is a direct solution of Maxwell's time-dependent curl equations [13]. The goal is to model the propagation of an electromagnetic wave into a volume of space containing a dielectric or conducting structure. By time stepping, i.e., repeatedly implementing a finite-difference

Manuscript received December 16, 1980; revised July 14, 1981. This work was supported by the Rome Air Development Center, Griffis Air Force Base, New York, and IIT Research Institute, Chicago, IL, under Contracts F30602-77-C-0613 and F30602-79-C-0039,

The authors are with the Electronics Division, IIT Research Institute, 10 West 35th Street, Chicago, IL 60616.

0018-926X/82/0700-0617$00.75 © 1982 IEEE

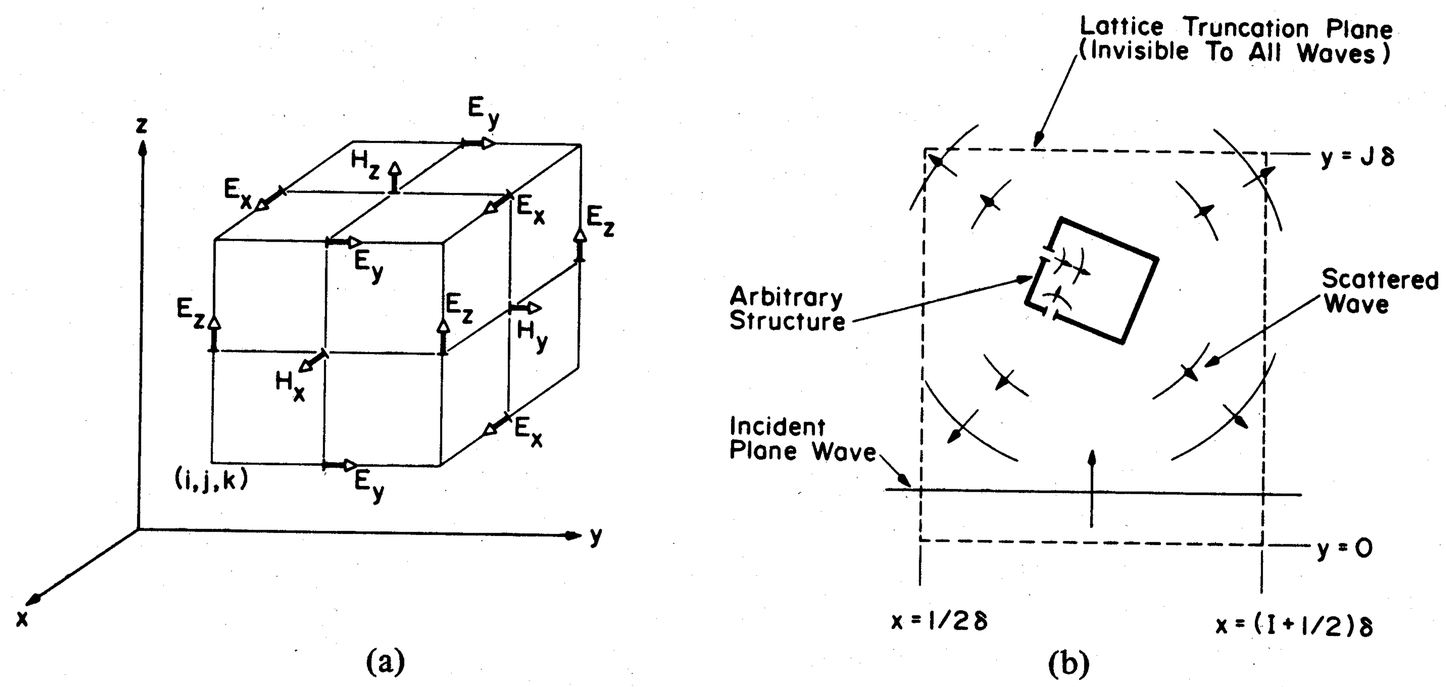

Fig. 1. (a) Positions of field components about a unit cell of Yee lattice [20]. (b) Ideal FD-TD lattice truncation conditions.

analog of the curl equations at each cell of the corresponding space lattice, the incident wave is tracked as it first propagates to the structure and then interacts with it via surface current excitation, diffusion, penetration, and diffraction. Wave tracking is completed when the desired late-time or sinusoidal steady-state behavior is observed at each lattice cell. Time stepping for the FD-TD method is accomplished by an explicit finite-difference procedure due to Yee [21]. For a cubic-cell space lattice [13], [20], this procedure involves positioning the components of $\vec{E}$ and $\vec{H}$ about a unit cell of the lattice as shown in Fig. 1(a) and evaluating $\vec{E}$ and $\vec{H}$ at alternate half-time steps. The centered difference expressions [13]–[16] can be used for both the space and time derivatives to attain second-order accuracy in the space and time increments [20]. The structure of interest is mapped into the space lattice by first choosing the space increment and then assigning values of permittivity and conductivity to each component of $\vec{E}$. In this manner, inhomogeneities or fine details of the structure can be modeled with a maximum resolution of one unit cell. Thin surfaces are modeled as stepped-edge sheets [20]. The following is a brief listing of key points on which pure FD-TD is based [13]–[16].

1) Lattice Truncation Conditions: The field components at the lattice truncation planes cannot be determined directly from the Maxwell's equations analog and must be computed using an auxiliary radiation [20] truncation condition. However care must be exercised because this condition must not cause excessive spurious reflection of waves scattered outward by the structure modeled. The goal is to formulate truncation planes as close as possible to the structure (to minimize computer storage), and yet achieve virtual invisibility of these planes to all possible waves within the lattice, Fig. 1(b).

2) Plane Wave Source Condition: The simulation of either an incident plane wave pulse or single-frequency plane wave should not take excessive storage or cause spurious wave reflections. The former would occur if the incident wave is programmed as an initial condition; the latter would occur if the incident wave is programmed as a fixed field excitation along a single lattice plane [13]–[16].

3) Sinusoidal Steady-State Information: Such data can be obtained either by a) directly programming a single-frequency incident plane wave or b) performing a separate Fourier transformation step on the pulse waveform response. Both methods require time stepping to a maximum time equal to several wave periods at the desired frequency. The second method has two additional requirements. First, a short rise time pulse suffers from accumulating waveform error due to overshoot and ringing as it propagates through the space lattice. This leads to a numerical noise component which should be filtered before Fourier transformation. Second, Fourier transformation of many lattice-cell field versus time waveforms (each probably extending over hundreds of time steps) would significantly add to the total requirements for computer storage and execution time [15], [16].

4) Total-Field Versus Scattered-Field Formulation: A choice exists in whether to finite-difference only the scattered field instead of the total field (at each lattice cell). The scattered-field approach may lead to a relatively superior lattice truncation condition [22]. However the total-field approach may be more useful in determining the fields penetrating structures having shielding properties, or the fields in the shadow regions of scatterers, where the total field can diminish to levels far below the incident. Scattered-field codes have traditionally run into numerical "noise" problems for such cases since they achieve interior or shadow-zone field reduction by the subtraction of nearly equal scattered and incident field quantities. Shielding or shadowing of more than 30 dB may be difficult to achieve in this manner because of a residual "noise" floor inherent in this computer subtraction process. A total-field approach does not suffer from the subtraction-noise problem and hence is suitable for computing field penetration within shielded structures or into shadow zones.

Previous work leading to this paper described efforts to solve the first three problems above for the case of a total-field FD-TD program employing a cubic-unit-cell space lattice [13], [16]. Simple truncation conditions were developed for two- and three-dimensional lattices that reduced the reflection coefficient of closely positioned truncation to the order of 0.1 for waves of arbitrary incidence. A plane wave source condition was described that allowed generation of an arbitrary pulsed or sinusoidal incident wave without requiring any additional storage and without causing spurious wave reflections, Fig. 1(b).

III. THE HYBRID TECHNIQUES

In order to treat the penetration and aperture coupling problems more effectively, a new hybrid MM/FD-TD technique has been developed based on a novel use of a field

equivalence theorem due to Schelkunoff [18]. This hybrid technique and its applications, described in this section, is basically an equivalent aperture excitation method. This allows analysis of the coupling problem in two steps.

Step 1: Analysis of the relatively simple exterior problem using MM to compute the equivalent excitation currents in the apertures leading to the interior region. This can be done *independent* of any knowledge of the contents of the interior region.

Step 2: Use of the FD-TD method to analyze the relatively complex interior region, assuming as an excitation the equivalent currents found in Step 1.

In this way, each analysis method is applied in the range of structure size and complexity for which it is best suited, allowing an overall solution that is accurate for large simple structures penetrated by apertures leading to complex interior cavities.

This section will review the following topics relevant to the use of the hybrid MM/FD-TD method: 1) the basis of the hybrid method; 2) limitations of potential hybrid MM/MM approaches; and 3) case studies of MM/FD-TD analyses.

A. Basis of the Hybrid Analyses Using the Third Schelkunoff Equivalence Theorem

Fig. 2 illustrates the classical problem of a perfectly conducting scatterer S_c with an aperture S_A. External to the scatterer in Region 1, an incident field $(\vec{E}^i, \vec{H}^i)$ illuminates the aperture, and part of the energy penetrates into the cavity (Region 2) through the aperture. To compute the total field $(\vec{E}_2, \vec{H}_2)$ in Region 2, many analytical and MM numerical approaches studied in the literature have employed integral-equation formulations treating Regions 1 and 2 simultaneously. These approaches characterize either S_A or S_c in terms of tangential aperture fields or equivalent surface currents [1]–[6], [11], [12], [23], [24].

An alternative approach is to employ a field equivalence theorem due to Schelkunoff ([18, theorem 3]) to permit sequential treatment of the penetration into Region 2. This theorem is based upon an equivalent aperture electric current formulation which connects the exterior and interior regions. This formulation expresses the fields in a region as the superposition of the so-called short-circuit field $(\vec{E}_{sc}, \vec{H}_{sc})$ with the aperture not present (shorted) plus the aperture field contribution $(\vec{E}^A, \vec{H}^A)$ maintaining the required continuity of the fields across the aperture. The first partial field $(\vec{E}_{sc}, \vec{H}_{sc})$ is simply equal to zero in the Region 2. The second partial field $(\vec{E}^A, \vec{H}^A)$ is generated by the nonphysical current distribution $\vec{J}^A$ flowing through the empty space of the aperture region where $\vec{J}^A = -\vec{J}_0{}^A$ the short-circuit aperture current distribution.

B. MM/MM Hybrid Analysis

Recently Schuman and Warren [8] have applied the Schelkunoff equivalence principle to interface the MM technique with MM to analyze the exterior and interior regions of an open-ended cylinder, and a nose-cone structure with a nose aperture and a thin circumferential gap aperture [8], [19], [20], [28]. Both the cylinder and nose-cone structures were treated as bodies of revolution. Their analysis was restricted only to *empty interior regions,* and their goal was to improve the accuracy of field computation for cases when the aperture coupling is small and/or points deep within the cavity are sought. This is possible because the hybrid method avoids any subtraction of nearly equal impressed and scattered fields to compute the total field within Region 2. Thus error due to residual subtraction noise is eliminated. The hybrid approach of Schuman and Warren is illustrated in Fig. 3 and is summarized below as a five-step computation.

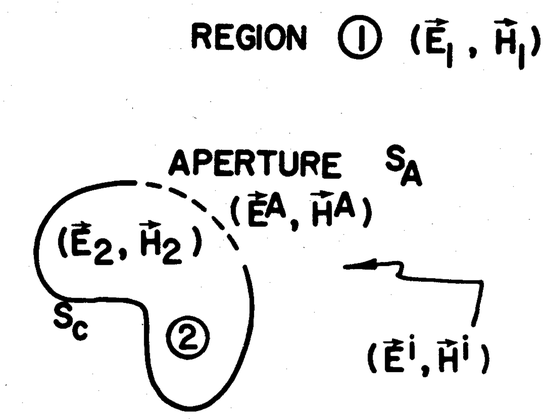

Fig. 2. Perfectly conducting scatterer with aperture.

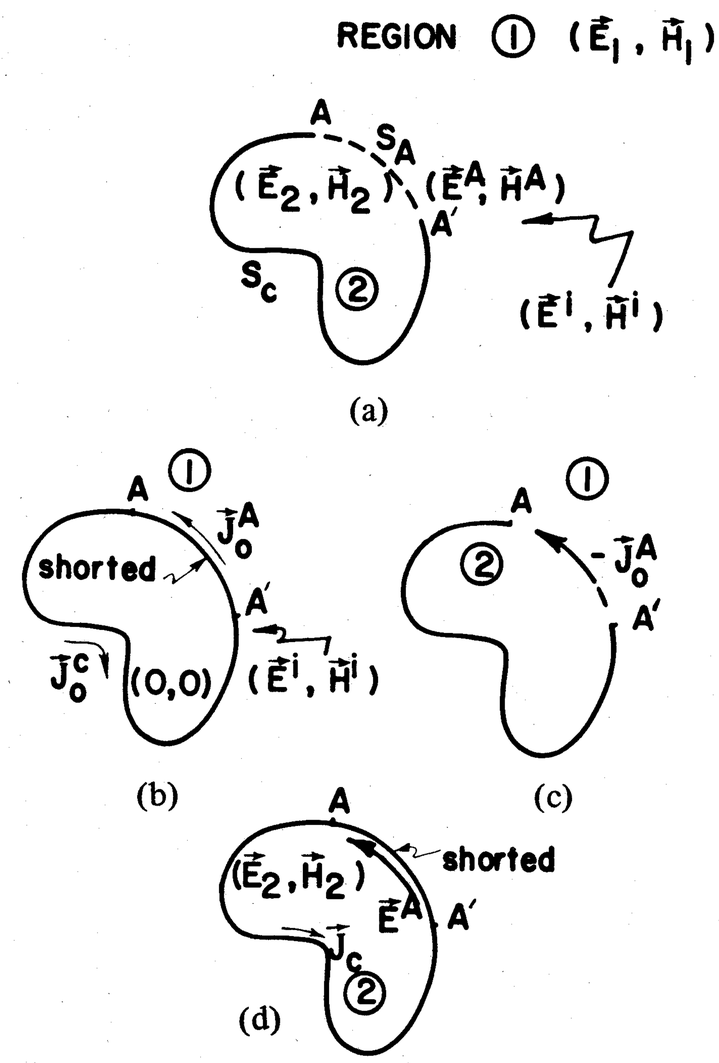

Fig. 3. MM/MM hybrid technique.

Region 1: MM Technique

a) The aperture region S_A is short-circuited, and the straightforward exterior problem is solved via MM [28], [29] to obtain the induced electric current distribution $\vec{J}_0{}^A$ in the short-circuited aperture region Fig. (3(b)).

b) The short-circuit current $\vec{J}_0{}^A$ is now placed in the open aperture region with a sign change (Fig. 3(c)) to account for the continuity of the fields in the aperture region [8], [18]. The electric current $-\vec{J}_0{}^A$ nonphysically placed in the open aperture region acts as an equivalent source for the fields in Region 1 and 2.

Region 2: MM Technique

c) Based on the generalized multiport approach [1], referring to the Region 2, an equivalent electric field excitation $\vec{E}^A$ existing only in the aperture region (Fig. 3(d)) is determined which will produce the electric current $-\vec{J}_0$ with the aperture short-circuited.

d) The electric current distribution $\vec{J}_c$ is obtained on the

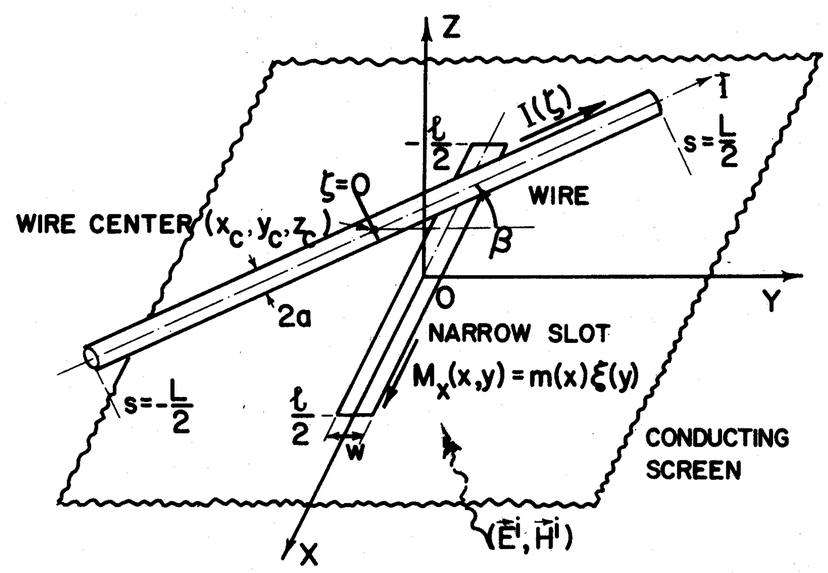

Fig. 4. Geometry of wire scatterer behind narrow slot [11].

interior surface of the conducting body with $\vec{E}^A$ as the equivalent source electric field (Fig. 3(d)).

e) The interior fields ($\vec{E}_2$, $\vec{H}_2$) are now computed based on $\vec{J}_c$ and $\vec{E}^A$ or $-\vec{J}_0{}^A$.

C. Limitations of MM/MM Hybrid Analyses

As pointed out by Schuman and Warren [8], any loading within the cavity region (Region 2) changes the aperture equivalent electric field excitation $\vec{E}^A$ of Step c) above. Therefore, the generalized multiport approach of Step c) must take into account any loading within the cavity by either metal or dielectric objects. This requirement introduces considerable complexity and perhaps explains why the MM approach has not been more widely used as a means of modeling realistic problems. This cavity loading effect is now discussed in more detail. We consider the [11], [12] problem illustrated in Fig. 4. A wire scatterer of length L and radius a is placed at a distance of z_c behind a narrow slot of length l and width w in a conducting screen of infinite extent. The center of the wire is located directly above the center of the slot on the z axis. Further, the slot is along the x axis and the angle between the wire and the slot bisector (the y axis) is defined as β. Excitation for this system is provided by the plane wave ($\vec{E}_y{}^i$, $\vec{H}_x{}^i$) propagating in the lower half-space ($z < 0$) at normal incidence to the screen. This problem was reported [11] with numerical results derived via a direct coupled integral equation and MM solution. Basically a coupled set of integro-differential equations [11], was derived by treating the aperture electric field and the wire electric current distribution as unknowns. The coupled equations were solved by expanding the unknown distributions in terms of standard pulse functions and then testing the resulting equations using piecewise triangular functions [1], [11].

Fig. 5 shows the results of the direct MM solution for a highly resonant coupled case. The electric field E_y in the slot is characterized in terms of an equivalent magnetic current distribution M_x in the shadow side:

$$\hat{y}E_y = \hat{x}M_x x\,\hat{z} \tag{1}$$

$$M_x = m(x)\xi(y) \tag{2}$$

where

m(x) axial distribution of the equivalent magnetic current in the slot

ξ(y) transverse distribution of the equivalent magnetic current in the slot

$$\xi(y) = \frac{1}{\pi}\left[\left(\frac{w}{2}\right)^2 - y^2\right]^{-1/2}. \tag{3}$$

In Fig. 5(a) the shadow side ($z = 0+$) slot axial magnetic current distribution $m(x)$ in the presence of the screen and the wire is plotted for $\beta = 0$. This angle corresponds to the wire axis being physically perpendicular to the slot axis, which is the orientation for maximum coupling between the slot and wire. Both real and imaginary parts of $m(x)$ are plotted. Fig. 5(b) shows the corresponding distribution of the induced electric current on the wire.

Now, consider the possibility of implementing the MM/MM hybrid solution presented in the previous section. To apply this technique the slot shown in the Fig. 4 is first short circuited by replacing the slot by a perfectly conducting material identical to the screen itself. Next the lower half-space $z < 0$ is analyzed as a pure boundary value problem. The induced electric current $\vec{J}_0{}^A$ on the shorted region of the slot is determined for the given plane wave excitation ($\vec{E}_y{}^i$, $\vec{H}_x{}^i$), as simply

$$\vec{J}_0{}^A = -2H_x{}^i\hat{y}. \tag{4}$$

Next we go back to the original problem and place in the open slotted region an equivalent aperture electric current excitation of

$$\vec{J}^A = \begin{cases} -\vec{J}_0{}^A \text{ or} \\ 2H_x{}^i\hat{y}. \end{cases} \tag{5}$$

The next step in the MM/MM hybrid technique is initiated by computing an equivalent aperture electric field excitation $\vec{E}^A$ which will produce the electric current $-\vec{J}_0{}^A$ with the aperture short circuited. When the slot and wire are uncoupled ($\beta = 90°$) $\vec{E}^A$ is found by treating the slot as a multiport generalized system [1], [8] and then inverting the system equation

$$[\bar{J}^A] = [\bar{\bar{Y}}^A][\bar{E}^A] \tag{6}$$

where

$[\bar{\bar{Y}}^A]$ slot generalized admittance matrix.

When the wire is oriented such that $\beta \neq 90°$, there is coupling between the wire and slot. For this case the multiport generalized system matrix of (6) should be modified [1], [8], [12] according to Fig. 6 yielding

$$[\bar{J}^A] = [[\bar{\bar{Y}}^A] + [\bar{\bar{Y}}_w{}^A]][\bar{E}_w{}^A] \tag{7}$$

where

$[\bar{\bar{Y}}_w{}^A]$ mutual generalized admittance matrix at the slot due to the presence of the wire (accounts for wire coupling; also known as the wire admittance loading matrix or transfer admittance matrix [12]).

and

$[\bar{E}_w{}^A]$ slot equivalent electric field excitation in the presence of the wire scatterer.

For the slot-wire geometry, the calculation of the $[\bar{\bar{Y}}_w{}^A]$ is

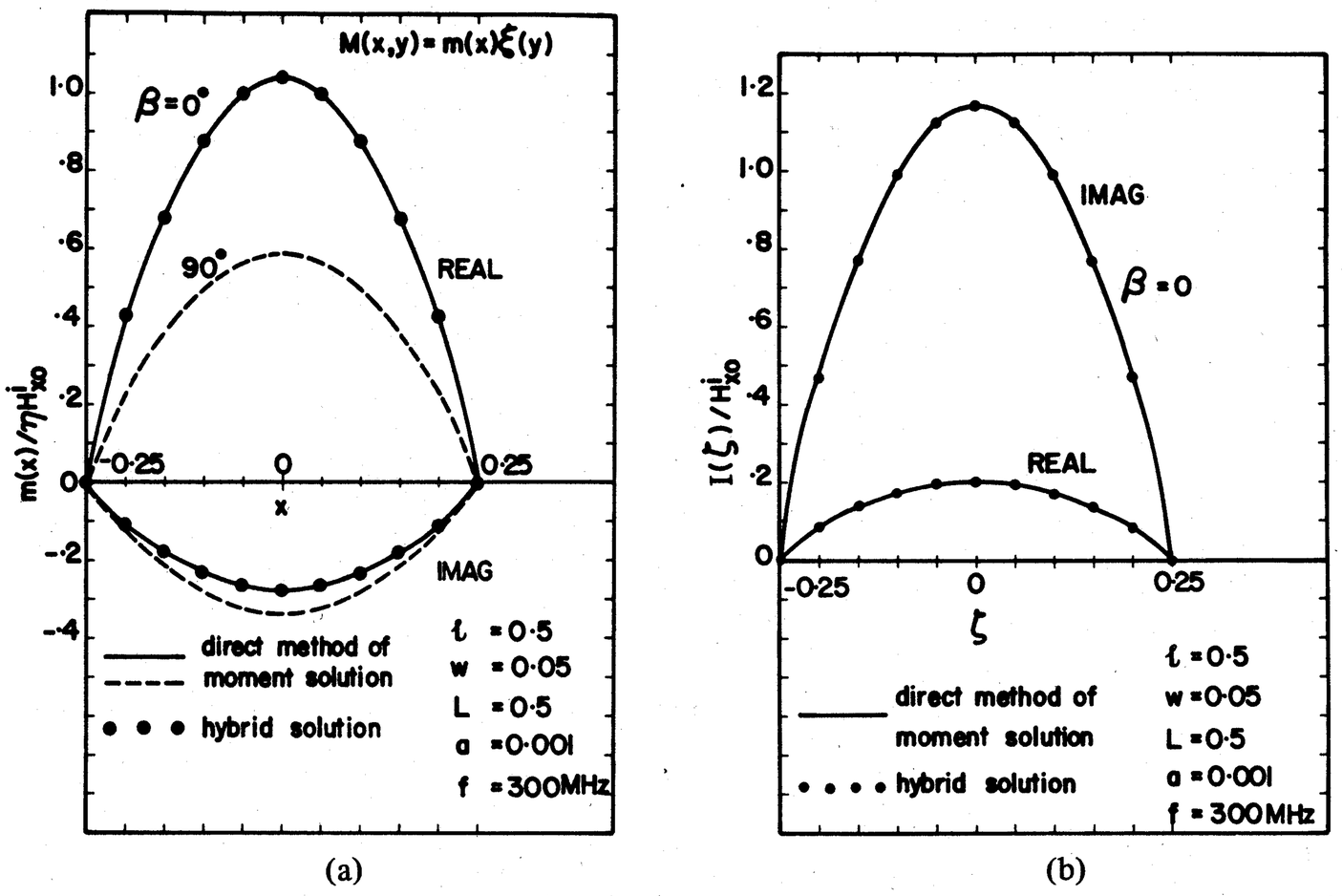

Fig. 5. Results of direct one-step MM and hybrid MM/MM solutions of geometry of Fig. 4. (a) Shadow-side slot magnetic current distribution. (b) Wire electric current distribution.

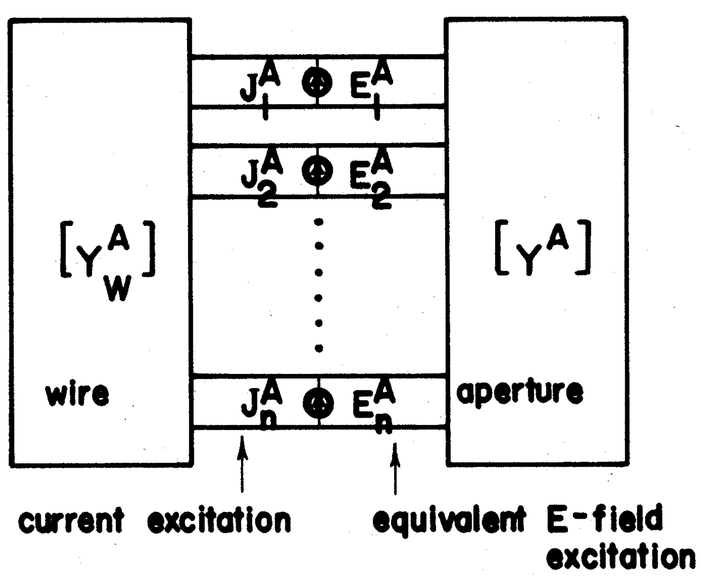

Fig. 6. Multiport generalized network representation for hybriding MM with MM.

straightforward [1] and in fact can be written in a closed form for very long wire scatterers [12].

The hybrid matrix equation (7) has been solved for $\beta = 0°$ for the canonical geometry of the Fig. 4, and the computed results for the slot distribution are plotted in Fig. 5(a). Excellent agreement with the direct integral equation solution is seen. The equivalent aperture electric field excitation radiates in the presence of screen, and electric current $I(\zeta)$ is induced on the wire by mutual coupling interaction. In Fig. 5(b), the computed electric current induced on the wire (based on the hybrid formulation) is plotted. Again excellent agreement with the results is obtained.

It is concluded that it is valid to apply Schelkunoff's third equivalence theorem [18] for apertures having wires closely coupled to them. It has been demonstrated that the resulting MM/MM hybrid approach is capable of dealing with such loaded apertures if the mutual interaction between the wire and the aperture is rigorously taken into account. However it is also clear that *any loading within the cavity region* changes the aperture equivalent electric field excitation $\vec{E}^A$. A generalized multiport approach similar to that of Fig. 6 must be used to take into account such loading by either metal or dielectric objects. This approach can prove extremely complex or even impossible to implement for general cavity regions since it involves computing the Green's function of the loaded cavity interior. Since this Green's function is also required for the direct integral equation and MM solution, there is little, if any, reduction of computational complexity when using the hybrid MM/MM approach for general cavities. If the material loaded cavity Green's function is calculable at all, the main advantages of the hybrid MM/MM approach over the direct MM approach lie in the enhanced stability and accuracy of the hybrid computations for cases where the interior fields are well below the incident fields.

D. MM/FD-TD Hybrid Analyses

In Fig. 7 the MM/FD-TD hybrid method is illustrated schematically and is summarized below as a four-step computation.

Region 1: MM Technique

a) Identical to step a) of the MM/MM method (Section III-B), Fig. 7(b).
b) Identical to step b) of the MM/MM method (Section III-B).

Region 2: FD-TD Technique

c) We note that the MM technique gives the equivalent current source distribution $-\vec{J}_0{}^A$ in the frequency domain as a spatial distribution of the phasor quantities having both magnitude (relative to the incident fields) and phase (relative to some phase reference, normally at the origin of the coordinate system). With the FD-TD method being a time-domain technique, the phase distribution of $-\vec{J}_0{}^A$ is interpreted as a time-delay distribution with respect to the original phase references location. The magnitude distribution is taken intact without interpretation or modification. In this manner the FD-TD aperture equivalent current source distribution assumes sinusoidal steady-state quantities starting at the very beginning of time stepping, with the proper time delay to account for phase shift.
d) Using the FD-TD approach the interior fields $(\vec{E}_2, \vec{H}_2)$ are computed directly by using $-\vec{J}_0{}^A$ as a source term distribution in the $\nabla X \vec{H}$ difference equations [20].

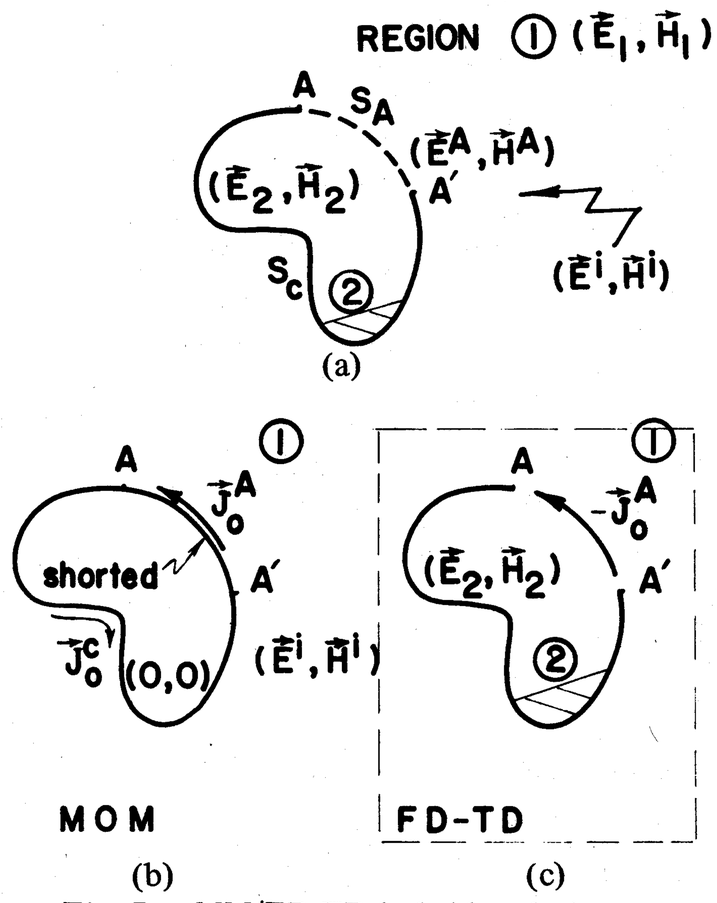

Fig. 7. MM/FD-TD hybrid technique.

Here, specifying $-\vec{J}_0{}^A$ in the aperture is equivalent to specifying a discontinuity in the tangential magnetic field across the aperture plane [18].

Note that, unlike the hybrid MM/MM method, the hybrid MM/FD-TD method does *not* require computation of the equivalent aperture electric field excitation $\vec{E}^A$. This is because the interior-region FD-TD solution easily accepts the nonphysical aperture electric current distribution $-\vec{J}_0{}^A$ as the excitation. Thus there is no need to set up and solve for the mutual interactions of the cavity contents and the apertures, and no need to compute the loaded cavity Green's function. The hybrid MM/FD-TD method easily permits the modeling of the cavity interior to as fine an extent as desired without any additional numerical complication.

E. Case Studies of MM/FD-TD Hybrid Analyses

Two case studies are now reported to permit assessment of the validity and accuracy of the MM/FD-TD hybrid method: 1) open-ended cylinder, axial incidence; and 2) loaded missile guidance section, axial incidence. The results indicate that this hybrid technique is valid and useful for these and similar structures.

1) Open-Ended Cylinder, Axial Incidence: The MM/FD-TD hybrid model for the axial-incidence open-ended aluminum cylinder (19-cm diameter and 68.5-cm long, as shown in Figs. 8 and 9) was run for 800 time steps (2.0 cycles of the incident wave at $f = 300$ MHz). The excitation consisted of data for the magnitude and phase of the electric current distribution over the locus of the short-circuited aperture (as required by Schelkunoff's third theorem) computed using a MM body-of-revolution code [27], [28].

Fig. 10 depicts the coordinate system used for the MM/FD-TD hybrid analysis of the open-ended cylinder. Fig. 11 graphs the MM modal coefficients for the radial and circumferential components of $\bar{J}_0{}^A$. (For clarity, only the magnitude is shown.) Since only the $m = 1$ mode is present, the equivalent aperture current is given by [28].

$$\bar{J}_0{}^A(t, \phi) = \hat{t} J_t(t) \cos\phi + \hat{\phi} j J_\phi(t) \sin\phi \qquad \text{A/m} \qquad (8)$$

for any point (t, ϕ) on the aperture.

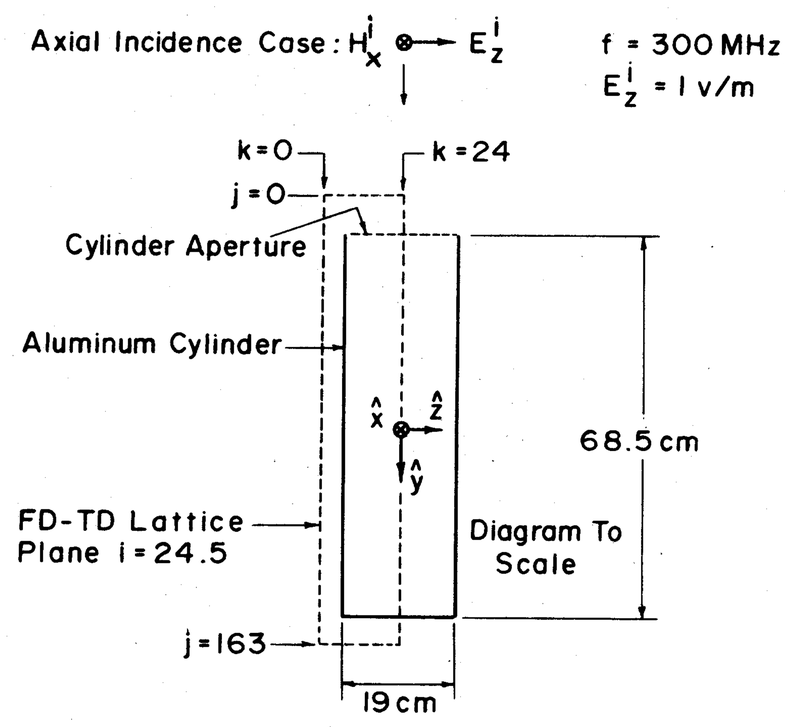

Fig. 8. FD-TD model geometry of open-ended aluminum cylinder, axial-incidence case as viewed at vertical symmetry plane.

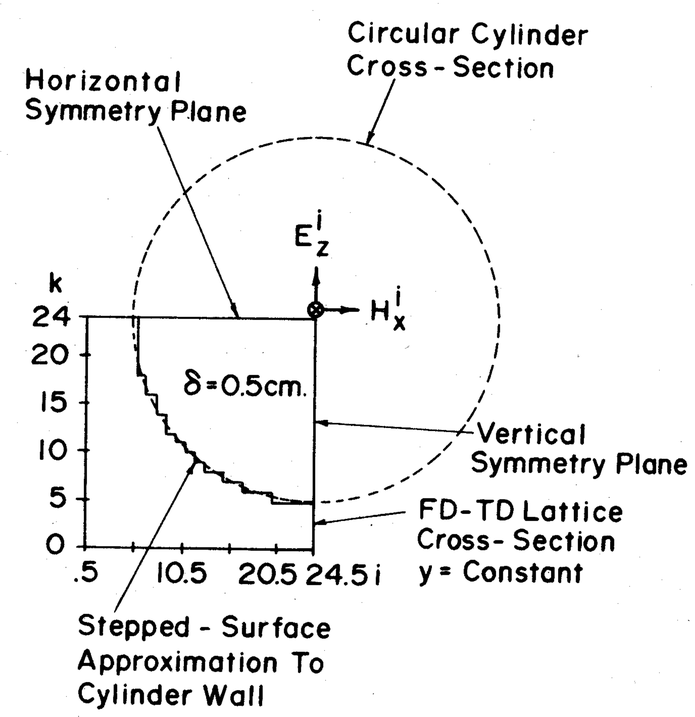

Fig. 9. Transverse cross section of cylinder model of Fig. 8.

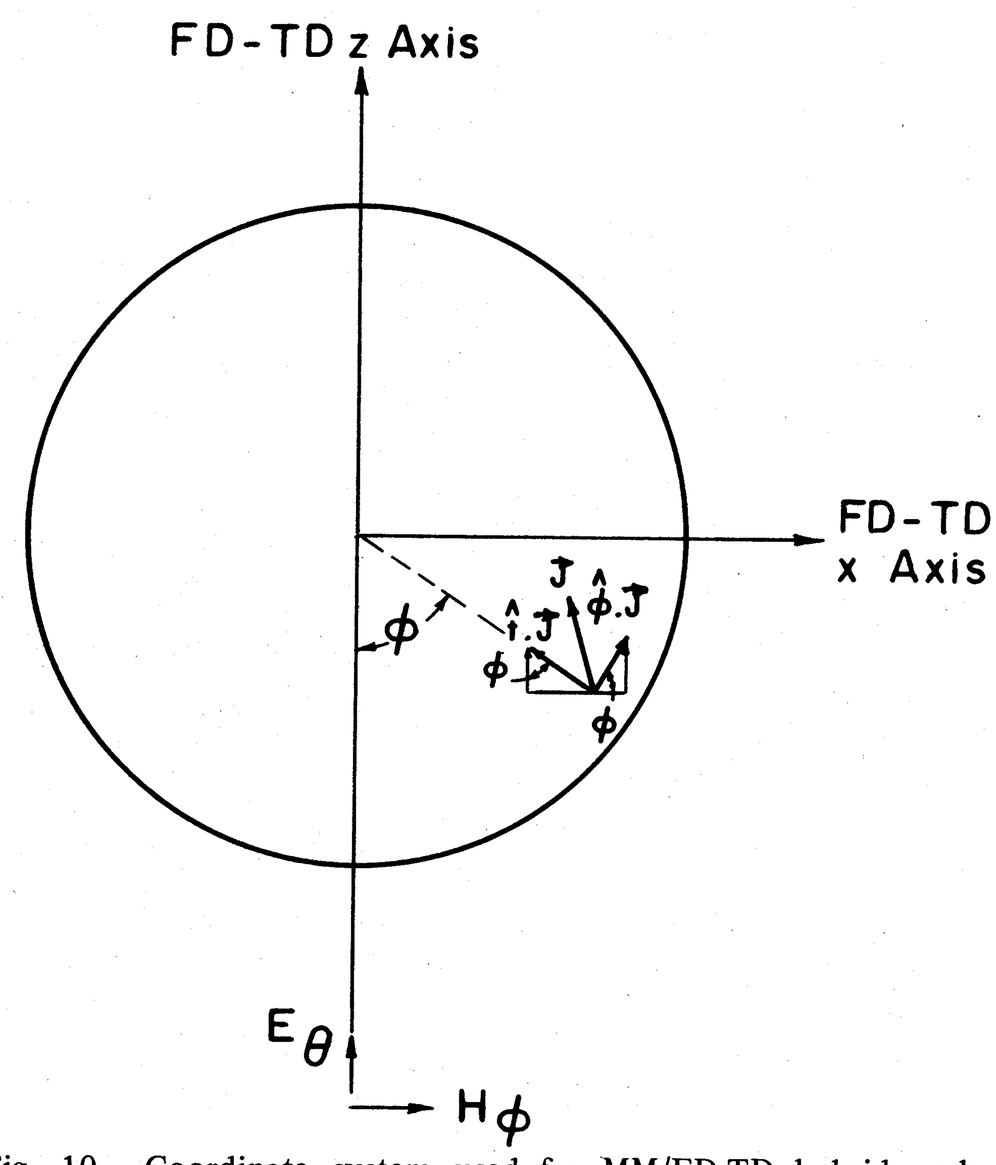

Fig. 10. Coordinate system used for MM/FD-TD hybrid analyses. Excitation for method of moments program; $\hat{t}$, $\hat{\phi}$—MM program coordinates; $\vec{J}$—surface current derived from MM program.

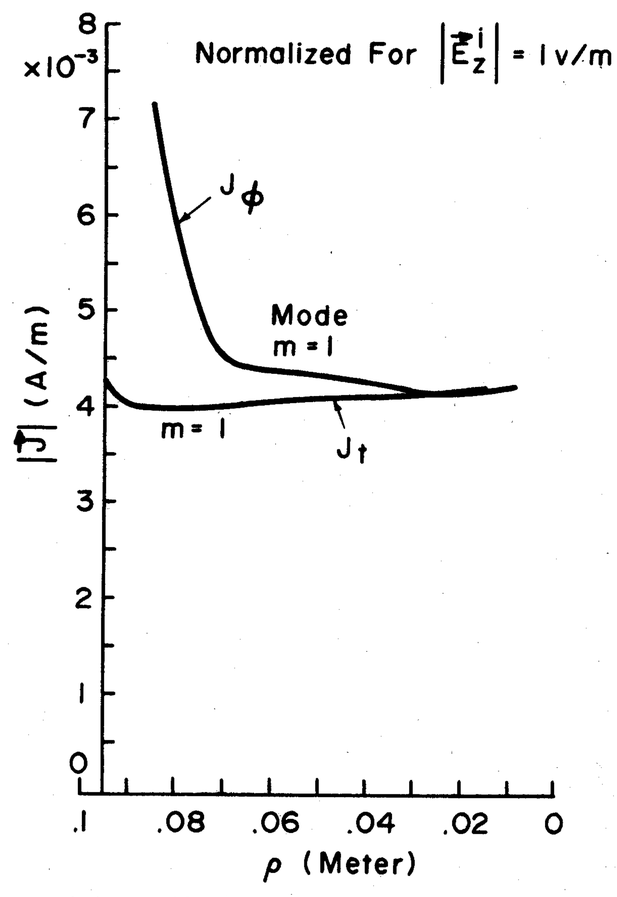

Fig. 11. MM modal coefficients of equivalent aperture current, axial-incidence cylinder case [20].

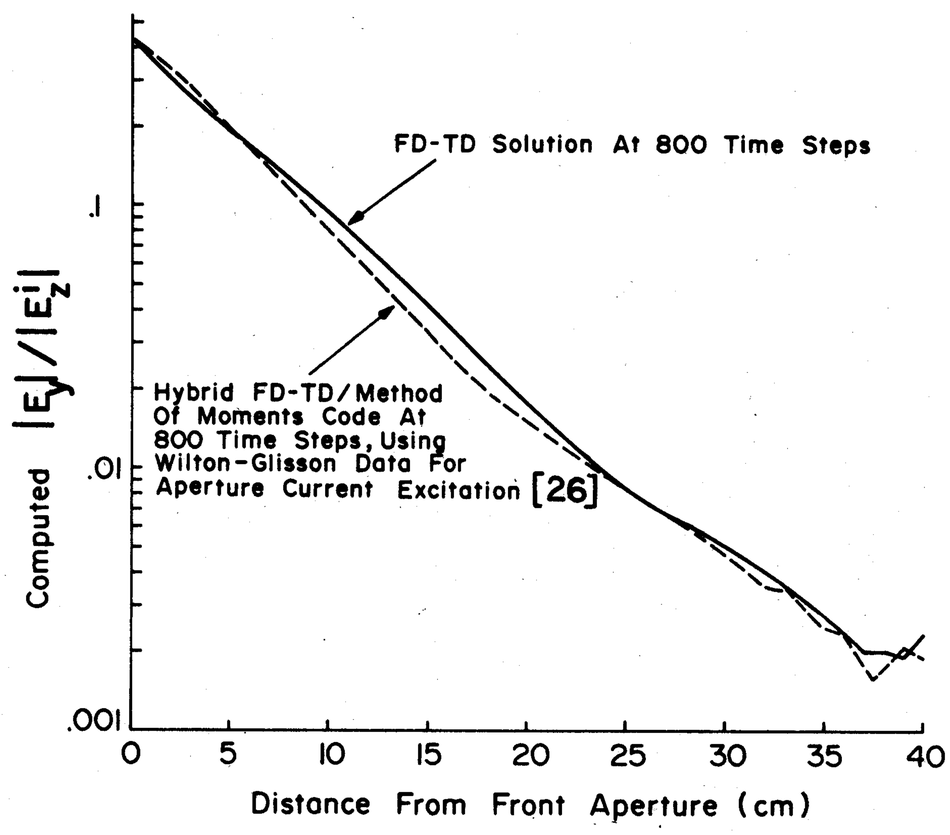

Fig. 12. Comparison of pure FD-TD and hybrid MM/FD-TD results for radial electric field along the axis of the cylinder of Figs. 8 and 9.

At all locations of E_x and E_z in the cylinder aperture, J_{0_x} and J_{0_z} were inserted as field equivalent sources via the $\nabla \times \vec{H}$ part of the FD-TD algorithm [20]. The FD-TD program was run for this excitation and the results were compared to previous pure FD-TD results for the axial-incidence open-ended cylinder.

Fig. 12 plots the comparison of the pure FD-TD results for the radial electric field along the cylinder axis with the hybrid MM/FD-TD program. It is seen that the results agree within approximately ± 1 dB up to 40 cm back from the aperture. Fig. 13 compares the computed field contours in the cylinder horizontal symmetry plane (as defined by Fig. 9) within 11 cm of the aperture. The maximum contour displacement is less than 1 cm indicating a very good agreement of the results.

The result of these comparisons is the conclusion that the MM/FD-TD hybrid approach yields data for this case (a 0.19–λ circular aperture in an elongated cylinder) that are *consistent* with previous data derived from both pure MM and pure FD-TD methods [20]. This is a significant agreement of three computational techniques based upon very different first principles.

2) Loaded Missile Guidance Section, Axial Incidence: The MM/FD-TD hybrid model for the axial-incidence case of the loaded guidance section [20] (as shown in Figs. 14 and 15) was run for 1800 time steps (3.0 cycles of the incident wave at $f = 300$ MHz). The excitation consisted of data for the magnitude and phase of the electric current distribution over the loci of the short-circuited nose aperture and sleeve-fitting aperture (as required by Schelkunoff's third theorem) computed using a MM body-of-revolution code [28]. The results were compared to pure FD-TD results presented [20] in an attempt to establish the consistency of the MM/FD-TD model for this case.

Fig. 16 plots the comparison of the hybrid MM/FD-TD results for the H field contours in the vertical symmetry plane with the pure FD-TD results [20]. It is seen that, for both methods stepped to 1800 time steps, there is an excellent agreement of the 0 dB contours near the wire connecting the cooled detector unit to the pre-amp can. For this contour the maximum spatial shift is only about 0.16 cm in a direction further out from the wire. Further, there is observed to be excellent agreement of the ±10 dB contour near the wire connecting the pre-amp can to the metal backplane. For this contour the maximum spatial shift is only about 0.1 cm in a direction further out from the wire. This implies that the current in these two major wires are predicted to be almost the same by both the pure FD-TD method and the hybrid MM/FD-TD method.

Fig. 17 plots the comparison of the hybrid results for the H_x and E_z fields along a vertical cut through the center of the guidance section at a point 21 cm in back of the nose aperture (about 2 cm in front of the sleeve fitting, at the point where the circumferential slot opens into the interior of the nose cone). The hybrid run results are after 1500 time steps, while the pure FD-TD results are after 1800 time steps. For this case a very high level of agreement is observed between the two sets of data at all points of comparison. The worst-case difference between the results is only 1 dB, with most results consistent within only fractions of a decibel.

Comparison of the data sets for the 1800 time-step case for each set results in slightly lessened agreement, such that the worst-case difference is about 1.7 dB. This may result from the hybrid program progressing to the sinusoidal steady state at a slightly faster rate than the pure FD-TD program, since a sinusoidal steady-state equivalent aperture current excitation is employed from the very beginning of the hybrid program, rather than an aperture excitation which must build to the steady state.

This case study shows that the hybrid MM/FD-TD approach yields results for the missile guidance section wire current and electromagnetic fields which are consistent with the pure FD-TD data. The study implies that a wire passing very close to an aperture, and strongly coupled to that aperture (as for the case of the pre-amp can-to-backplane wire near the sleeve-fitting aperture), can be consistently modeled using the pure FD-TD approach and the hybrid MM/FD-TD approach. In the latter, it must be remembered that the MM-derived equivalent aperture excitation takes into account *none* of the interior details of the structure. Finally the study implies that complex subsections of elongated simply-shaped structures are prime candidates for detailed modeling of the interior penetrating fields via the hybrid MM/FD-TD method.

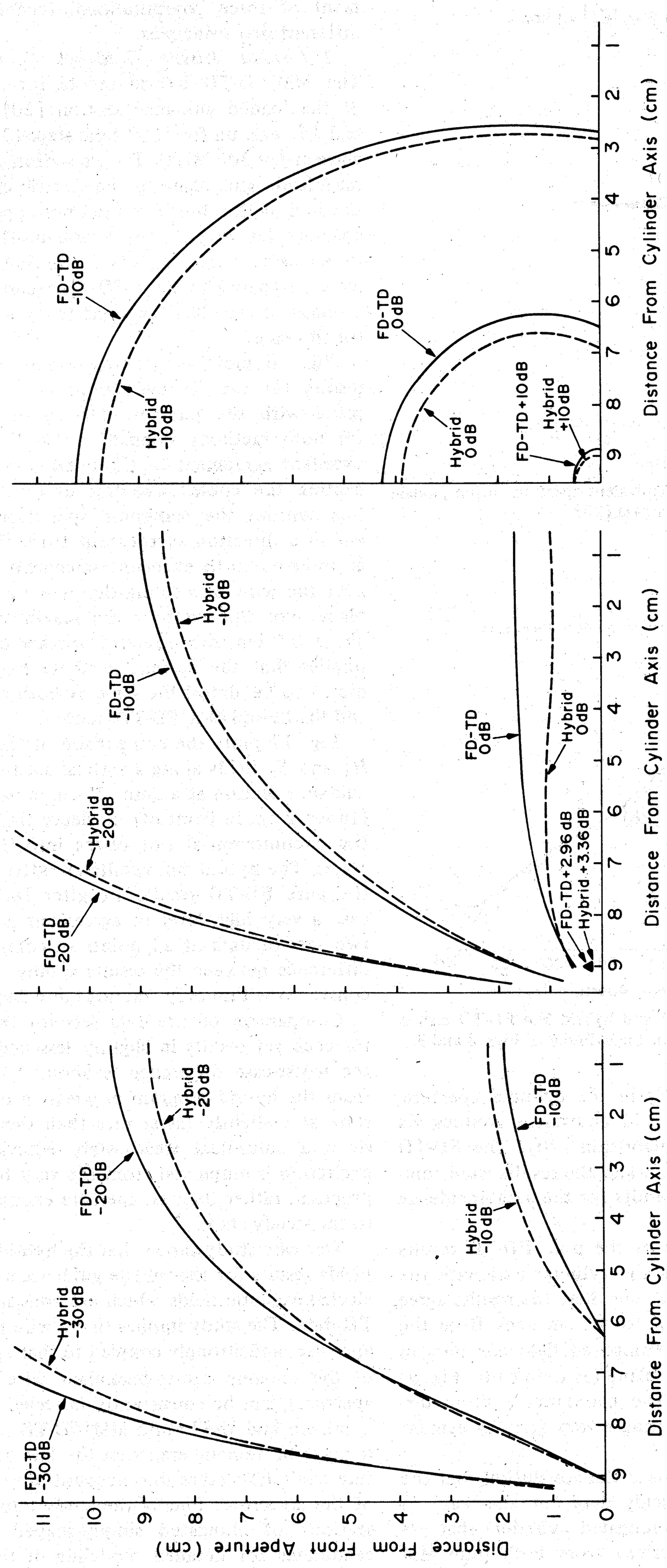

Fig. 13. Comparison of pure FD-TD and hybrid MM/FD-TD results for field contours in horizontal symmetry plane of cylinder of Figs. 8 and 9. (a) E_z. (b) H_x. (c) H_y.

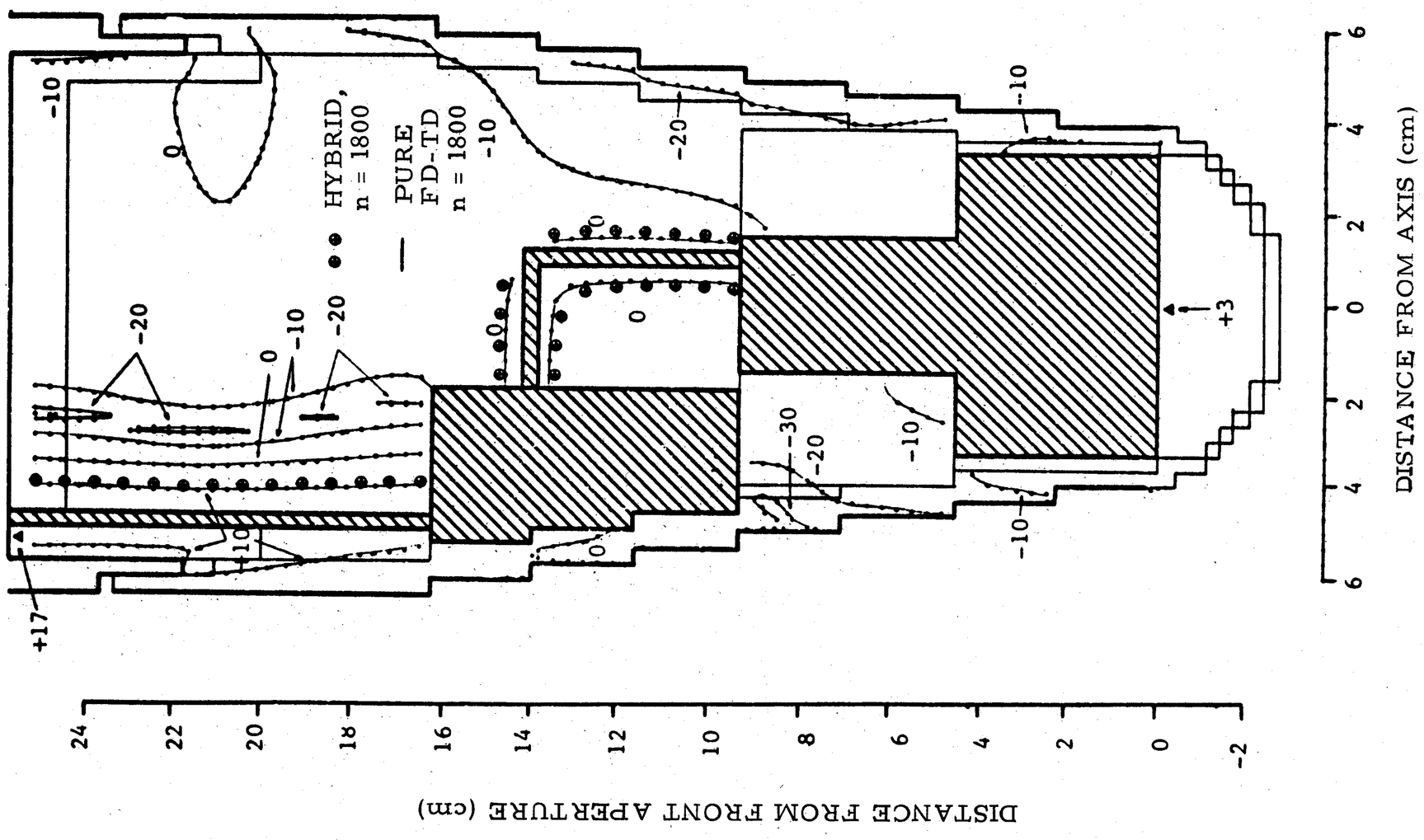

Fig. 16. Comparison of pure FD-TD and hybrid MM/FD-TD results for guidance section case, H_x field contours in vertical symmetry plane.

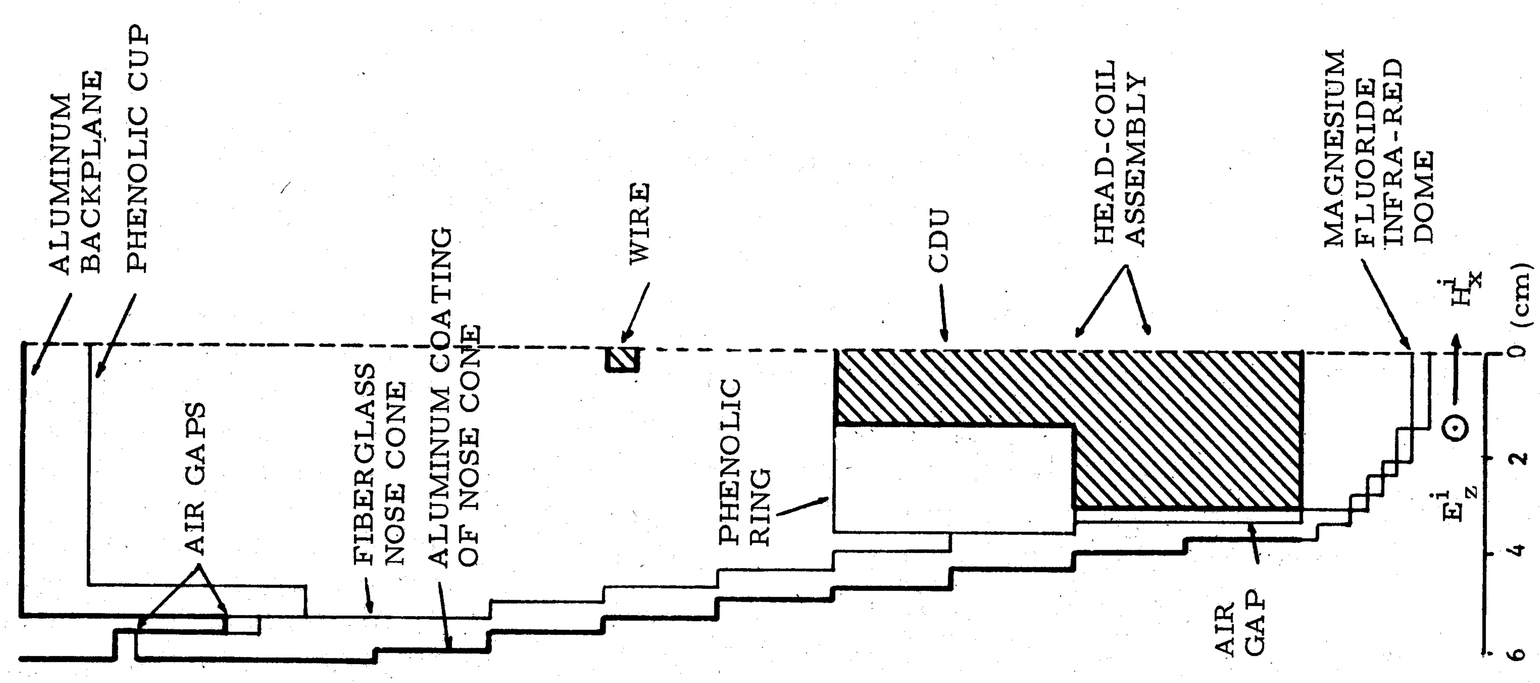

Fig. 15. Geometry of guidance section model at horizontal observation plane.

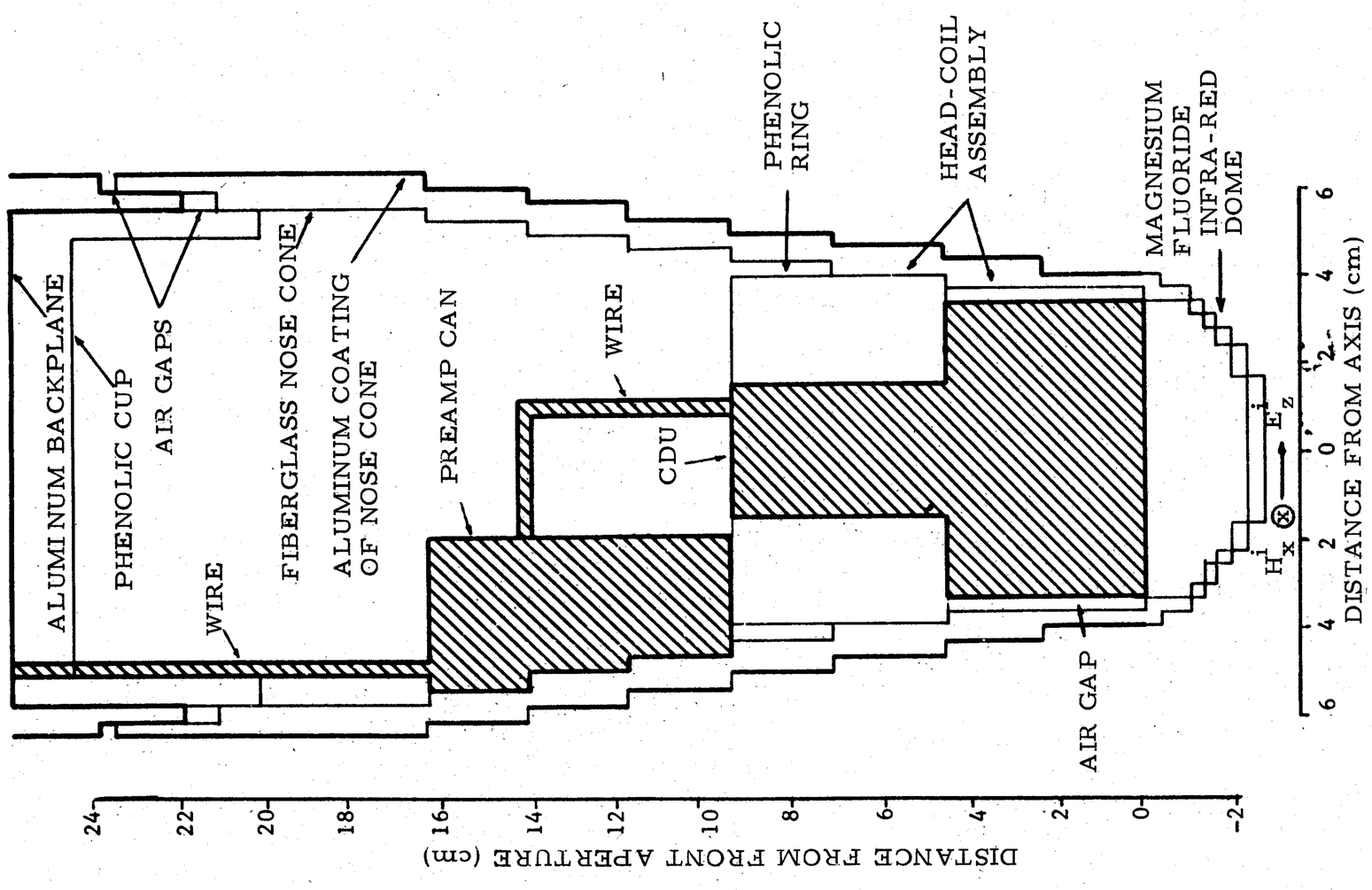

Fig. 14. Geometry of guidance section model at vertical symmetry plane, showing component materials.

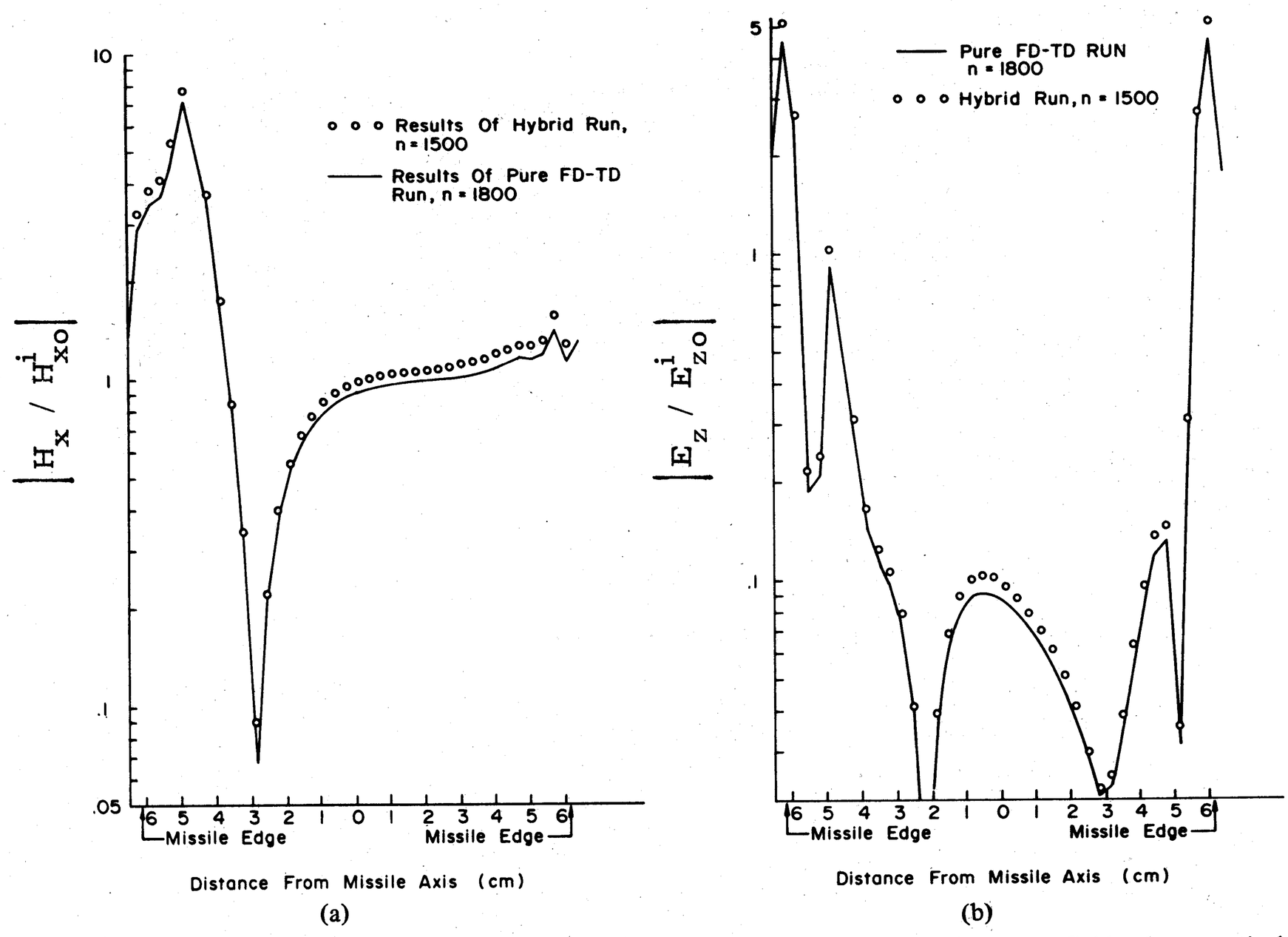

Fig. 17. Comparison of pure FD-TD and hybrid MM/FD-TD results, guidance section case, fields along vertical cut through the center near sleeve-fitting aperture. (a) H_x. (b) E_z.

IV. DISCUSSION AND CONCLUSION

This paper reviewed the application of the hybrid MM/FD-TD method to electromagnetic penetration and coupling problems involving conducting structures with potentially complex interiors. The FD-TD method [13]–[16] gives evidence of the capability of solving for more than 10^6 unknown field components within a localized space region, with an accuracy level in the order of ±1 dB and a ±1 lattice cell. Computer central processor times in the order of five minutes are required for such solutions when using available array processors such as the Control Data Star 100 and Cyber 203.

The hybrid MM/FD-TD method, based upon Schelkunoff's aperture electric current equivalence theorem, gives evidence of the capability of sequentially solving complex exterior/interior or global/local problems. This hybrid approach can take advantage of the ability of MM to solve exterior problems and easily account for arbitrary wave polarization and angle of incidence. The hybrid approach can also take advantage of the ability of FD-TD to model in great detail localized space regions containing metal structures, dielectrics, permeable media, anisotropic or nonlinear media, as well as wires. Overall, the hybrid MM/FD-TD method shows promise for the analysis of wave interaction with structures that require resolution of both large and small details at the same time.

REFERENCES

[1] R. F. Harrington, *Field Computation by Moment Methods*. New York: MacMillan, 1968.

[2] C. J. Bouwkamp, "Theoretical and numerical treatment of diffraction through a circular aperture," *IEEE Trans. Antennas Propagat.*, AP-18, no. 2, pp. 152–176, Mar. 1970.

[3] K. R. Umashankar and C. M. Butler, "A numerical solution procedure for small aperture integral equations," Interaction Note 212, July 1974.

[4] D. R. Wilton and O. C. Dunaway, "Electromagnetic penetration through apertures of arbitrary shape: Formulation and numerical solution procedure," Interaction Note 214, July 1974.

[5] D. R. Wilton, C. M. Butler, and K. R. Umashankar, "Penetration of electromagnetic fields through small apertures in planar screens: Selected data," Interaction Note 213, Sept. 1974.

[6] C. M. Butler and K. R. Umashankar, "Electromagnetic penetration through an aperture in an infinite planar screen separating two half spaces of different electromagnetic properties," *Radio Sci.*, vol. II, no. 7, July 1976.

[7] T. B. A. Senior and G. A. Desjardins, "Field penetration into a spherical cavity," Interaction Note 142, Aug. 1973.

[8] H. K. Schumann and D. E. Warren, "Aperture coupling in bodies of revolution," *IEEE Trans. Antennas Propagat.*, vol. AP-26, no. 6, pp. 778–783, Nov. 1978.

[9] K. R. Umashankar and C. E. Baum, "Transient electromagnetic characterization of arbitrary conducting bodies through an aperture—Perforated conducting screen," Interaction Note 343, Mar. 1978.

[10] C. E. Baum, "EMP simulators for various types of nuclear EMP environments: An interim categorization," Sensor and Simulation Note 151, July 1972.

[11] C. M. Butler and K. R. Umashankar, "Electromagnetic excitation of a wire through an aperture perforated conducting screen," *IEEE Trans. Antennas Propagat.*, vol. AP-24, no. 4, pp. 456–462, July 1976.

[12] K. R. Umashankar and J. R. Wait, "Electromagnetic coupling in an infinite cable placed behind a slot perforated screen," *IEEE Trans. Electromagn. Comp.*, vol. EMC-20, no. 3, pp. 406–411, Aug. 1978.

[13] A. Taflove and M. E. Brodwin, "Numerical solution of steady-state electromagnetic scattering problems using the time-dependent maxwell's equations," *IEEE Trans. Microwave Theory Tech.*, vol. MTT-23, pp. 623–630, Aug. 1975.

[14] ——, "Computation of electromagnetic fields and induced temperatures within a model of the microwave-irradiated human eye," *IEEE Trans. Microwave Theory Tech.*, vol. MTT-23, pp. 888–896, Nov. 1975.

[15] A. Taflove, "Time domain solutions for electromagnetic coupling," Rome Air Development Center, Griffiss AFB, Rome, NY, with IIT Research Institute, Chicago, IL, Final Rep. RADC-TR-78-142, Contract F30602-77-C-0163, June 1978.

[16] ——, "Application of the finite-difference time-domain method to sinusoidal steady-state electromagnetic-penetration problems," *IEEE Trans. Electromagn. Compat.*, vol. EMC-22, pp. 191–202, Aug. 1980.

[17] R. Holland, "Threde: A free-field EMP coupling and scattering code," *IEEE Trans. Nucl. Sci.*, vol. NS-24, pp. 2416–2421, Dec. 1977.

[18] S. A. Schelkunoff, "Field equivalence theorems," *Comm. Pure Appl. Math.*, vol. 4, pp. 43–59, June 1951.

[19] A. Taflove and K. Umashankar, "A hybrid FD-TD/MoM approach to the electromagnetic coupling and aperture penetration," in *Proc. North America Radio Sci. Meeting* (URSI), PQ, Canada, p. 94, June 2–6, 1980.

[20] A. Taflove, "Evaluation of time domain electromagnetic coupling techniques," IIT Research Institute, Chicago, IL, Final Rep. RADC-TR-80-251 to Rome Air Development Center, Griffiss AFB, NY, Contract F30602-79-C-0039, 1980.

[21] K. S. Yee, "Numerical solution of initial boundary value problems involving Maxwell's equations in isotropic media," *IEEE Trans. Antennas Propagat.*, vol. AP-14, pp. 302–307, May 1966.

[22] D. E. Merewether, "Transient currents induced on a metallic body of revolution by an electromagnetic pulse," *IEEE Trans. Electromagn. Compat.*, vol. EMC-13, pp. 41–44, May 1971.

[23] E. K. Miller and A. J. Poggio, "Moment-method techniques in electromagnetics from an application viewpoint," in *Electromagnetic Scattering*, P. L. E. Uslenghi, Ed. New York: Academic, ch. 9, 1978.

[24] C. D. Taylor, D. H. Lam, and T. H. Shumpert, "Electromagnetic pulse scattering in time-varying inhomogeneous media," *IEEE Trans. Antennas Propagat.*, vol. AP-17, pp. 585–589, Sept. 1969.

[25] J. A. Stratton, *Electromagnetic Theory*. New York: McGraw-Hill, 1941, pp. 563–573.

[26] D. Wilton and A. Glisson, Univ. Mississippi, private communication to A. Taflove.

[27] H. K. Schuman and D. E. Warren, "Coupling through rotationally symmetric apertures in cavities of revolution," Rome Air Development Center, Griffiss AFB, NY, Rep. RADC-TR-77-214, June 1977.

[28] A. W. Glisson and D. R. Wilton, "Simple and efficient numerical techniques for treating bodies of revolution," Rome Air Development Center, Griffiss Air Force Base, NY, Rep. RADC-TR-79-22. Mar. 1979.

[29] J. R. Mautz and R. F. Harrington, "Radiation and scattering from bodies of revolution," *Appl. Sci. Res.*, no. 20, pp. 405–435, 1969.

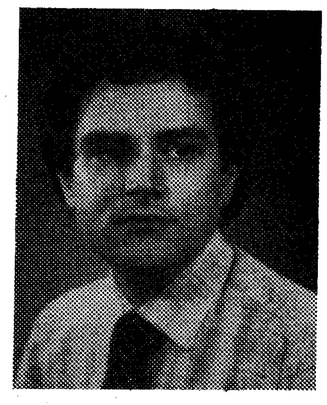

Allen Taflove (M'75), was born in Chicago, IL, on June 14, 1949. He received the B.S., M.S., and Ph.D. degrees from Northwestern University, Evanston, IL, in 1971, 1972, and 1975, respectively, all in electrical engineering.

In 1975, he joined the IIT Research Institute (IITRI), Chicago, IL. Currently, he is a Senior Engineer in the EM Technology Section, responsible for applied electromagnetics research. His research has been concerned with electromagnetic wave penetration and scattering, low-frequency coupling of earth-return transmission-line systems, and the development of novel techniques for the recovery of fuels from oil shale and tar sand based upon *in situ* radio-frequency heating. He has been granted five foreign and two U.S. patents for his *in situ* fuel recovery inventions.

Dr. Taflove is a member of Eta Kappa Nu, Tau Beta Pi, Sigma Xi, and the American Association for the Advancement of Science.

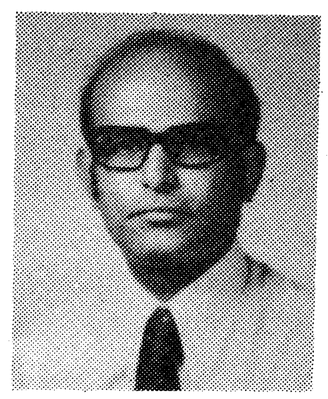

Korada Umashankar (S'69–M'75–SM'81), received the B.E. degree from Mysore University, India in 1962, the M.E. degree from Indian Institute of Science, Bangalore, India in 1964, and the Ph.D. degree from University of Mississippi, University, in 1974, all in electrical engineering.

From 1964 to 1969, he was Assistant Professor of Electrical Engineering at College of Engineering, Karnatak University, Hubli, India. During 1974–1975 he was a Post-Doctoral Research Associate, and during 1975–1977, he was Assistant Professor of Electrical Engineering in the Department of Electrical Engineering, University of Mississippi. From 1977–1979, he was the National Research Council Visiting Fellow at the Airforce Weapons Laboratory, Kirtland AFB, Albuquerque, NM, involved with the simulator studies and electromagnetic transients. Presently, he is with the electromagnetic section of the IIT Research Institute, Chicago, IL. His primary research work has been in the development of analytical and mathematical techniques in electromagnetic theory, EMP interaction, and EM simulation studies.

Dr. Umashankar is a member of Sigma XI and Eta Kappa Nu.